Carbohydrate Research, 248 (1993) 303–316
Elsevier Science Publishers B.V., Amsterdam

Progressive dissociation of pectin

M.L. Fishman *, P. Cooke, A. Hotchkiss and W. Damert

U.S. Department of Agriculture †, ARS, Eastern Regional Research Center, 600 East Mermaid Lane, Philadelphia, PA, 19118 (USA)

(Received February 26th, 1993; accepted May 26th, 1993)

ABSTRACT

The structural organization of alkaline soluble peach pectin was investigated over size ranges extending from micrometers to tenths of nanometers. Analysis was by electron microscopy and high-performance anion-exchange chromatography (HPAEC). Superimposed and individual circular microgels in the micrometer size range were isolated from mesocarp tissue of cell walls and visualized by rotary shadowing. Dilute NaCl and 50% aqueous glycerol disaggregated these microgels into rods, segmented rods, and kinked rods, which collectively comprised the internal gel network of the microgels. Image analysis of the shadowed specimens before and after disaggregation followed by curve fitting of the smoothed distributions revealed a multimodal distribution of lengths. HPAEC revealed that the multimodal aggregates were stable for the most part to further dissociation by increasing ionic strength.

INTRODUCTION

Pectin is a group of complex anionic polysaccharides that consist primarily of blocks of α-(1 → 4)-linked D-galacturonyl residues (acid and methylester forms) interrupted by (1 → 2)-linked L-rhamnosyl residues. Neutral sugar side chains, primarily arabinogalactans, are also present[1]. The primary structure has been studied extensively because pectin is important as (1) a structural and functional component in the cell walls of higher plants, (2) a soluble food fiber with significant nutritional benefits, and (3) a substantial source of texture in fresh and processed fruits and vegetables[2]. Nevertheless, much less is known about higher orders of structure (i.e., secondary, tertiary and quarternary) and how these orders might affect items 1–3. Recently[3], we have visualized circular microgels of pectin (about one micrometer in diameter) isolated from cell walls of peaches and demonstrated that their internal gel structure was comprised of rods, segmented

* Corresponding author.

† Reference to a brand or firm name does not constitute an endorsement by the U.S. Department of Agriculture over others of a similar nature not mentioned.

rods and kinked rods. We believe that these microgels are held together to a large extent by hydrogen bonds because the gels could be dissociated into their component parts by treatment with NaCl or aqueous glycerol. Furthermore, the distribution of structural components (rods, etc.) was multimodal and comparable with sizes of particles measured by HPSEC. The multimodal and possibly periodic nature of the lengths of pectin aggregates suggests an intricate subunit structure for pectin.

In this work we extended the size range over which pectin structures were investigated. We also propose and test a simple rule for the dissociation of the hydrogen bonded internal structure of pectin gels, apply nonlinear least squares curve fitting to quantitate component lengths of subunit[5] visualized by microscopy, and propose a model for the progressive dissociation of pectin gels.

EXPERIMENTAL

Pectin.—Cell walls were obtained from the mesocarp of the hard, melting flesh of "Redskin" peaches which were harvested 140 days after the tree flowered (1 week prior to tree-ripe maturity). The cell walls were extracted with 50 mM *trans*-1,2-diaminocyclohexane-*N*,*N*,*N'*,*N'*-tetraacetic acid (CDTA) and sodium acetate (pH 6.5) for 6 h at 25°C (ref 4). The insoluble residue was collected on a sintered glass filter and then extracted with 50 mM $NaCO_3$ containing 2 mM CDTA for 20 h at 4°C, followed by 1 h at 25°C. The carbohydrate solubilized from the residue, termed alkaline soluble pectin (ASP), was exhaustively dialyzed against distilled, deionized water, and lyophilized. ASP contained 85.8% of galacturonic acid, expressed as a percentage of total ASP sugar content. Total sugar content was determined by the phenol–H_2SO_4 method[5], whereas galacturonic acid as a percentage of total sugar was determined by Scott's method[6].

Pectin hydrolysis.—ASP (10 mg) was incubated in 1 mL of 0.1 M NaCl, pH 4.4 at 39°C to which 1 unit of purified *endo*-polygalacturonase[7] was added. Hydrolysis was stopped after 30 min by raising the pH to 7 and heating to near boiling for 10 min in a water bath.

HPSEC.—Global and subunit values of contour lengths as determined by high-performance size-exclusion chromatography with refractive index detection were taken from a previous publication[3].

HPAEC.—High-performance anion-exchange chromatography was performed as previously described[8]. The solvent delivery system was a Dionex Bio-LC equipped with a pulsed amperometric detector II (PAD II, gold electrode). The mobile phase consisted of a 100 min nonlinear concentration gradient of potassium oxalate, pH 6 (25–500 mM). Pectic oligosaccharides were separated on a CarboPac PA1 (4 × 250 mm) column with a CarboPac PA1 guard column in line.

Transmission electron microscopy (TEM).—Lyophilized ASP was prepared for transmission microscopy by dissolving in water, 50% aq glycerol solution, 5 mM NaCl, 50 mM NaCl, or 50 mM ammonium acetate at concentrations of 10 and 100

μg/mL. Aliquots (10 μL) were sandwiched between freshly cleaved pieces of mica (2 cm^2), and after setting for 10–30 min, the sandwich was peeled apart and the mica was vacuum dried for 60 min at 5×10^{-6} torr, rotary shadowed with platinum at an angle of 5–8 degrees, and coated with a thin layer of carbon. The coated replicas were floated off the mica onto water, mounted on grids and examined by TEM in a Ziess 10B electron microscope.

Image analysis.—Rotary-shadowed images were recorded on photographic film at an instrumental magnification of 18000×, as measured from the average spacings of a replica grating with 54000 lines/in. Visible particles representing pectin in photographic prints (magnification 40000×) were traced onto a transparent overlay with a marking pen. Over 97% of the visible particles were traced. The tracings were digitized, analyzed for contour lengths and converted to histograms (bin size was 10 nm) using Imageplus software in a Dapple Systems (Sunnyvalle, CA) image analyzer.

Curve fitting.—Histograms of particle frequency (counts) against length were converted to continuous distributions by a combination of data smoothing and curve fitting. The count (N_i) of molecules in the histogram was smoothed to (N_{is}) by adding one half of the incremental change between the values of (N_i) in adjacent bins to the lower bin value according to eq. (*1*) (ref 9).

$$N_{is} = N_i + \Delta N_i/2 \qquad (1)$$

The values of N_{is} were smoothed globally by fitting them to an envelope generated by a sum of overlapping Gaussian peaks, although the main reason for curve fitting was to identify the subunits of pectin[3]. The fit was obtained interactively with a nonlinear regression program. The standard deviations (σ) of all peaks were set equal. The initial estimate of σ was obtained from the almost totally resolved peak at ~210 nm in Figs. 8–9. Estimates of number of peaks, heights and locations were also made from visual observations. These variables were iterated to a best fit convergence with the aid of the curve-fitting program which used a least-squares criterion for goodness of fit. The value of σ at convergence was 13 nm. The iteration technique was the Gauss–Newton method slightly modified[10]. In essence, the program minimizes the sum of the squares of the residuals between the N_{is} values and the expected values of the frequencies. The curve-fitting program, ABACUS, was developed "in-house" and is coded in FORTRAN. Copies of the program can be obtained by writing to the authors.

RESULTS AND DISCUSSION

Images in Figs. 1–5 show the effect of solvents on the quarternary structure of pectin. Initially we describe these images qualitatively, then quantitate the size distribution of subunits in microgels before and after dissociation and finally propose a mechanism for the dissociation of microgels and their subunits.

When concentrated aqueous solutions of pectin (ca. 100 μg/mL) were dried on mica, they formed flattened, discontinuous sheets composed of interconnected,

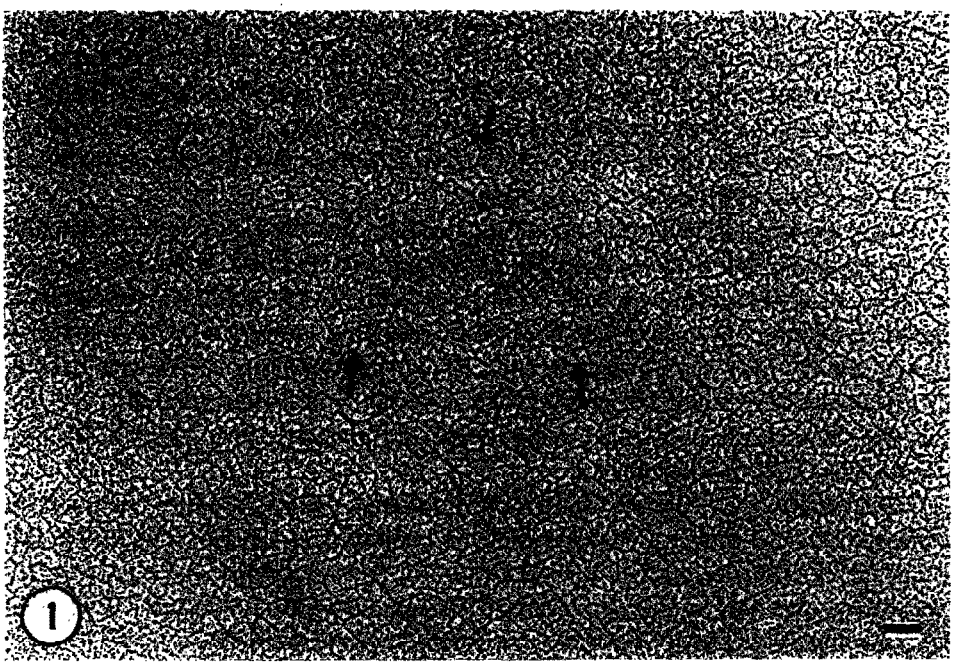

Fig. 1. Portion of a sheet of pectin network dried from water at high concentration (100 μg/mL). Arrows indicate interconnected subunits of rodlike, segmented rodlike, and kinked rodlike components which define open polygonal spaces.

curvilinear strings or subunits (Fig. 1). The widths of the subunits were less < 5 nm, and the lengths ranged from ~ 20 to > 300 nm. The arrangement of interconnecting subunits created an open network of polygonal spaces. Some isolated subunits with lengths that matched the range of lengths found within the network were found at the edges of the discontinuous sheets.

When dilute aqueous solutions of pectin (ca. 10 μg/mL) were dried on mica, they formed discrete, flat circular disks, ~ 1 μm in diameter. The disks contained the same type of open polygonal network with interconnected subunits that was found at high pectin concentrations (Fig. 2), and separate subunits were found at the circumference of the disks.

When dilute solutions of pectin in 50% aqueous glycerol were dried on mica, networks were no longer observed; instead, isolated subunits were found (Fig. 3). These varied in length but were uniform in width and were shaped either like rods, segmented rods, or kinked rods. Often, entire microscopic fields of these subunits were uniformly distributed and preferentially orientated on their mica substrates.

When dilute solutions of pectin in aqueous NaCl were dried on mica, once again, networks were no longer observed. In 5 mM NaCl mostly small clusters of interconnected subunits were observed in addition to a few isolated subunits (Fig. 4a), whereas in 50 mM NaCl only a few small isolated subunits were found (Fig.

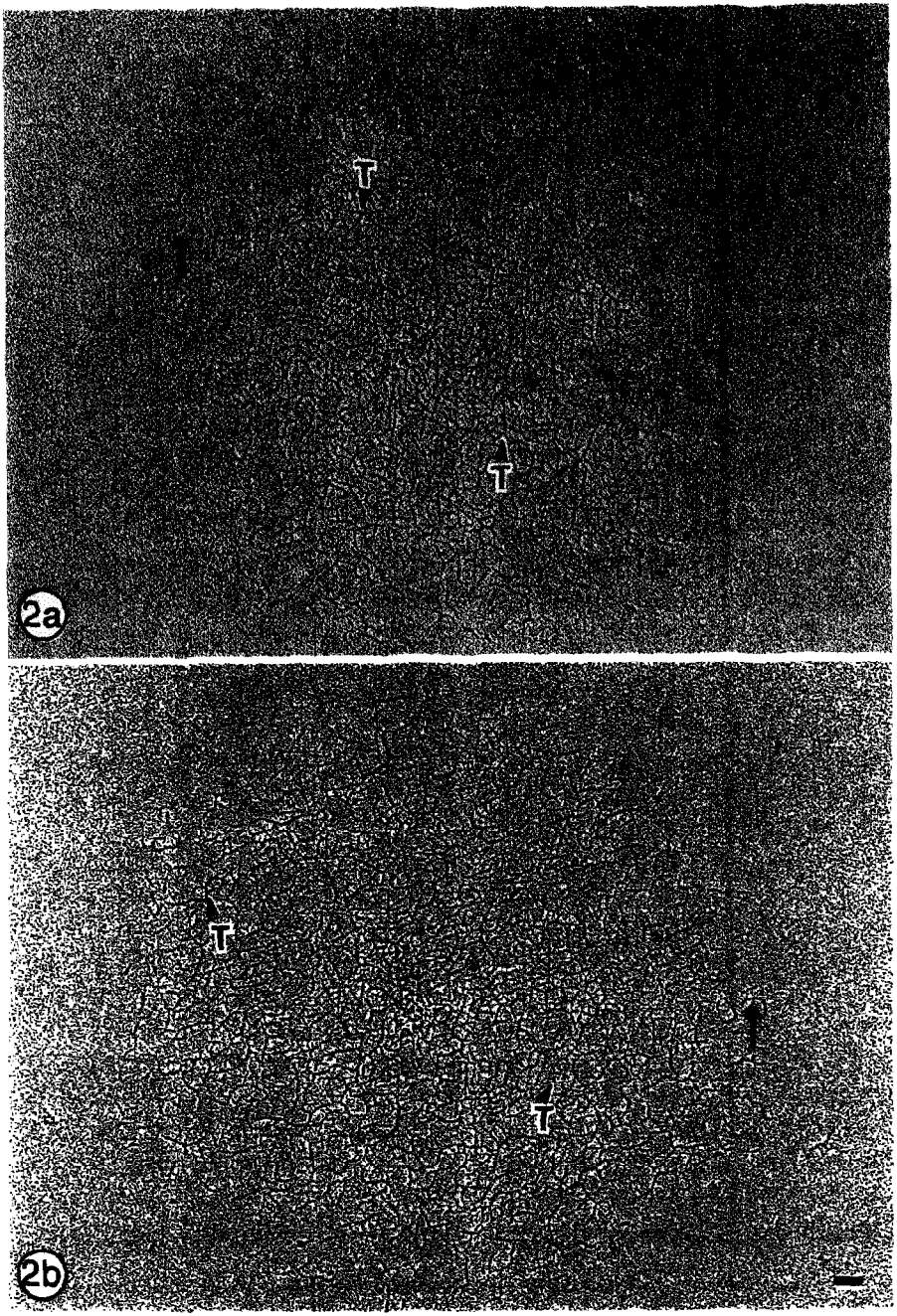

Fig. 2. Circular microgels of pectin (a and b) dried from water at low concentration (10 μg/mL). Similar subunits interconnect through T-junctions (T) to form open networks. Some isolated subunits (arrows) were located at the periphery of the microgels.

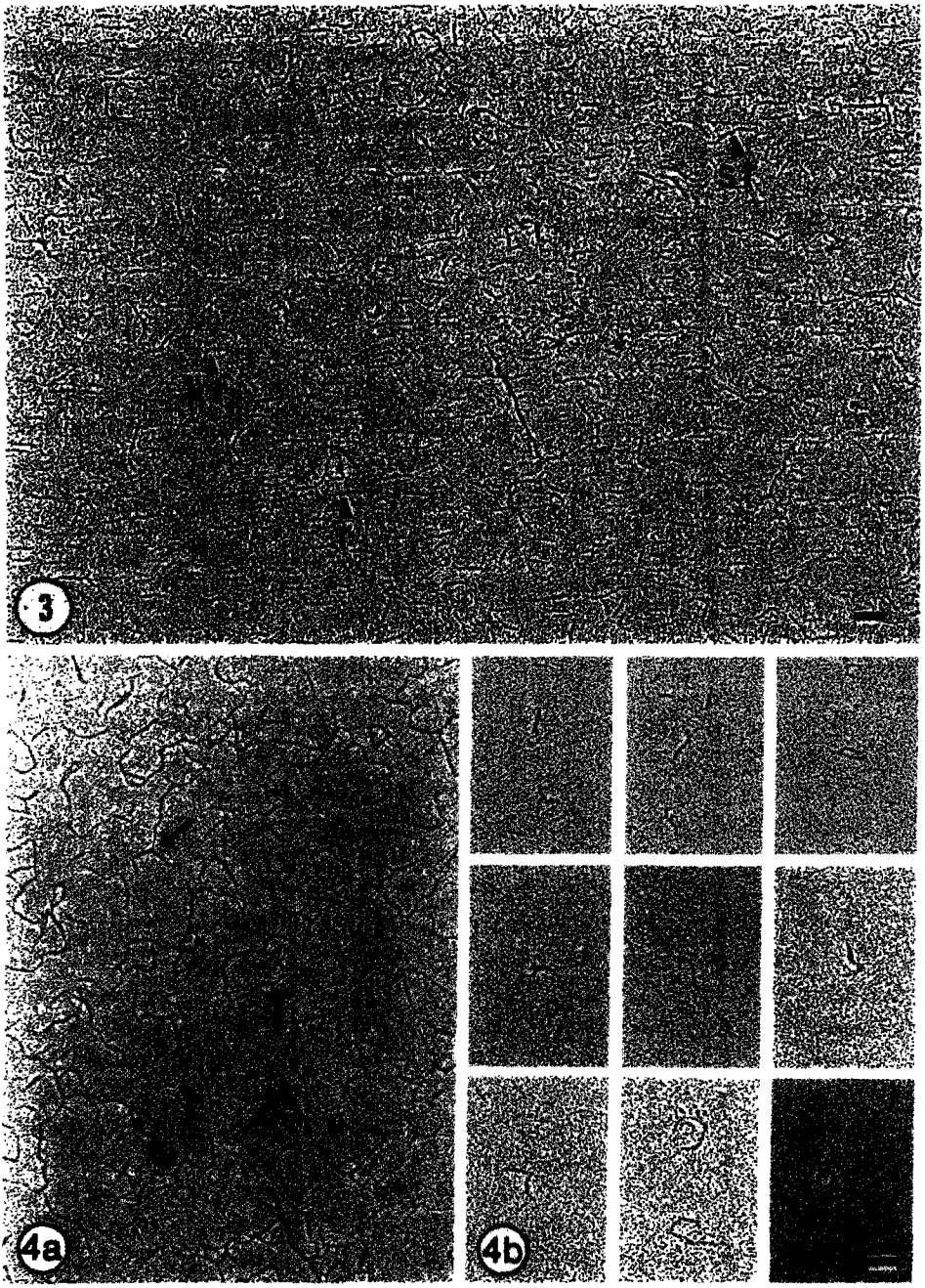

Fig. 3. Oriented dispersions of dissociated subunits shaped like rods (r), segmented rods (sr), and kinked rods (kr) of pectin (10 μg/mL), dried from 50% aqueous glycerol.

Fig. 4. (a) Partially dissociated subunits of pectin (10 μg/mL) had characteristic lengths but variable widths (arrows) when dried from 5 mM NaCl solution, and (b) montage of dissociated rods, segmented rods, and kinked rods of pectin (10 μg/mL), dried from 50 mM NaCl.

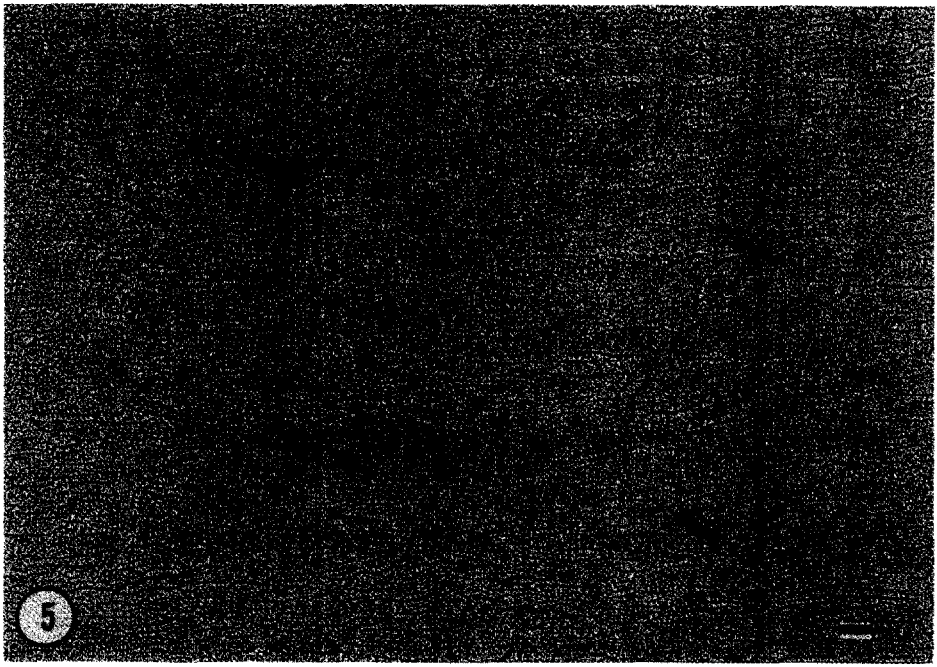

Fig. 5. Open oriented network of uniform thin pectin subunits in a sample of pectin (10 μg/mL) dried from 50 mM ammonium acetate. A small number of obliquely oriented subunits (arrows) connecting subunits oriented in parallel appears to have generated a gel with organization different from gels that were dried from water.

4b). The subunits dried from both NaCl solutions were comparable in length to those found along with the circular microgels and those dried from the glycerol solution. Widths of the various subunits dried from NaCl, but particularly from 5 mM NaCl, were variable and less than when prepared from either water or glycerol.

When dilute solutions of pectin in 50 mM ammonium acetate were dried on mica, a uniform and continuous network consisting of oriented and sparsely interconnected thin rods, segmented rods, and kinked rods was observed (Fig. 5), indicating that this solvent, unlike aqueous glycerol or salt, was capable of altering the density and orientation of chains within the gel network of pectin without permanently disrupting the network. We point this out to demonstrate that care must be taken when rotary shadowing pectin from aqueous solvents containing solutes capable of hydrogen bonding. For example, proteins are often rotary shadowed from aqueous solutions containing both glycerol and ammonium acetate.

In water, pectin may associate through hydrogen bonds at T-shaped junction points located at rhamnose inserts in the pectin backbone. Rhamnose is reported to be linked at the 1, 2, and 4 positions in pectin[11]. When not involved in glycosidic linkages, oxygen and hydrogen atoms at these positions could participate in hydrogen bonding. To test the hypothesis that pectin dissociates at junctions,

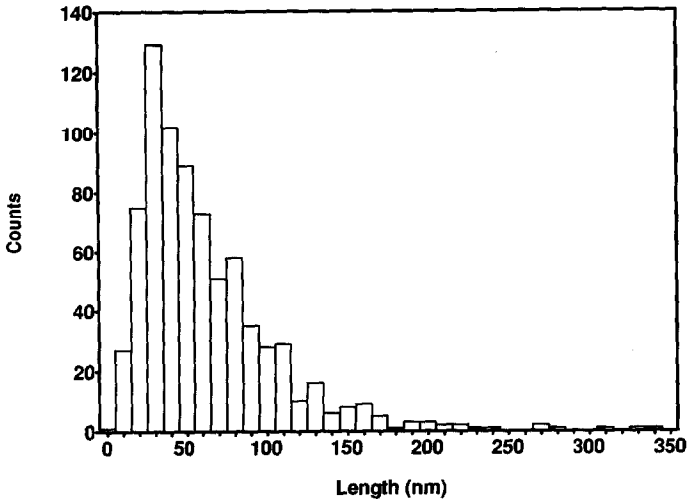

Fig. 6. Histogram of pectin component contour lengths from intact circular microgels. Obtained by analysis of images in Fig. 2.

pectin contour lengths were traced on transparent overlays from intact microgels such as shown in Fig. 2. Traced lines ended when joined at T-shaped junction points or at points of nonattachment. A histogram traced from images in an intact microgel is shown in Fig. 6, whereas a comparable histogram obtained from pectin dissociated in aqueous glycerol is shown in Fig. 7. The histogram in Fig. 6 was based on 771 objects as compared to 1502 objects for the histogram in Fig. 7. It is not readily apparent from these histograms whether the distribution of observed

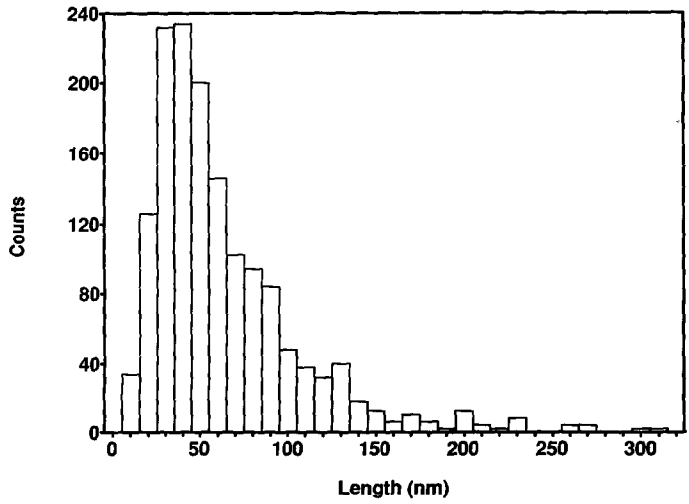

Fig. 7. Histogram of pectin subunits dissociated from microgels. Obtained by analysis of images in Fig. 3.

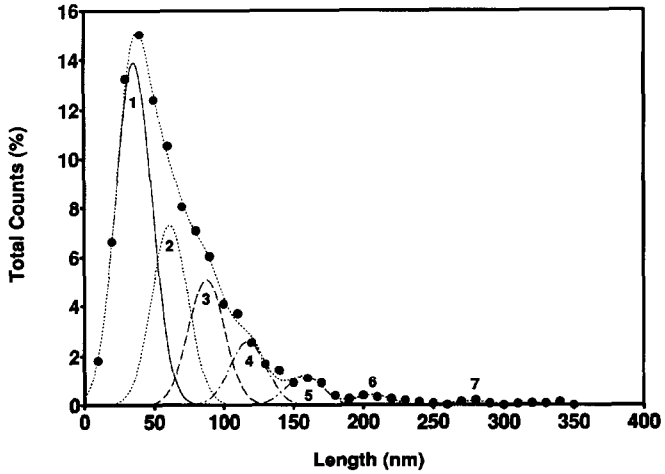

Fig. 8. Multimodal distribution obtained from smoothing and curve-fitting data in Fig. 6. Quarter bandwidth (σ) of Gaussian components is 13 nm. Numbers refer to components under heading "Microscope" in Table I.

objects is continuous or multimodal in nature. After smoothing and curve-fitting as discussed in the experimental section, the expected envelopes (dotted lines through points in Figs. 8 and 9) reveal the multimodal nature of the distributions. In our previous visual analysis[3] of data for glycerol dissociated pectin that was smoothed but not curve fitted, we did not recognize that the envelope peak at ~ 40 nm (Fig. 9) was in fact two unresolved peaks. Table I contains the contour lengths of pectins

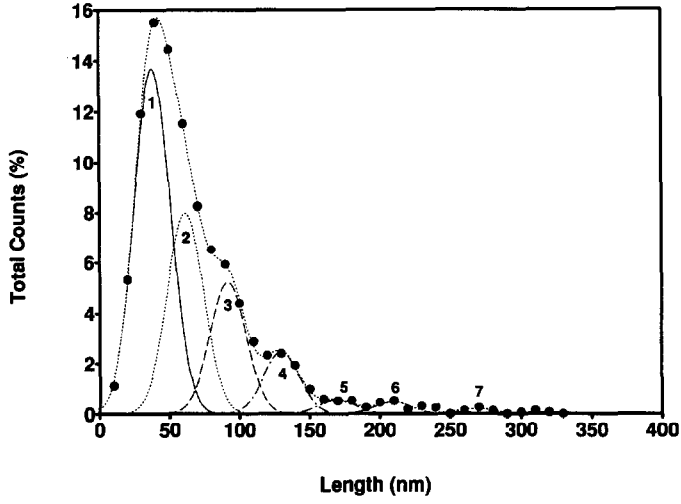

Fig. 9. Multimodal distribution obtained from smoothing and curve-fitting data in Fig. 7. Quarter bandwidth (σ) of Gaussian components is 13 nm. Numbers refer to components under heading "Microscope" in Table I.

TABLE I

Contour lengths of pectin components

Component		Length (nm)		
Microscope	HPSEC	Microscope	Microscope	HPSEC
		Water [a]	Water–Glycerol [b]	NaCl [c]
	4			27
1	3	36	38	44
2	2	61	61	77
3	1	87	92	150
4		117	130	
5		158	169	
6		207	210	
7		278	269	

[a] Measured by image analysis on intact microgels by assuming dissociation at T-junctions. Components 1–7 correspond to numbered peaks in Fig. 8. [b] Measured by image analysis on dissociated microgels. Components 1–7 correspond to numbered peaks in Fig. 9. [c] Calculated from R_g in 0.05 M NaCl by assuming rodlike behavior. HPSEC data taken from Table III in ref 3.

at the peak maximum of the fitted components. Also included in Table I are contour lengths obtained from HPSEC[3] in 0.05 M $NaNO_3$ by assuming that pectin is rod shaped. Comparison of component lengths visualized from undissociated (water) and dissociated (water–glycerol) preparations revealed fairly good agreement between comparable components in the two preparations. Comparison of distributions in Figs. 8 and 9 reveals similar shapes but somewhat better resolution in the dissociated preparation. Nevertheless by assuming the simple rule that the interior network of intact circular microgels (Fig. 2) dissociates at T-shaped junction points, we were able to obtain the contour length distribution of rods and segmented rods shown in Fig. 8 by making tracings as described above. This distribution was similar to the distribution of contour lengths in Fig. 9, which was obtained from tracings of the rods and segmented rods dissociated by aqueous glycerol as exemplified by the images shown in Fig. 3.

Comparison of microscopic lengths with those from HPSEC revealed fairly good agreement between comparable components 1 and 3 determined by the microscope and HPSEC, respectively, but increasingly poorer agreement between the two techniques was shown as contour lengths increase. (Note: components were numbered from left to right as they appear in the data output of the two respective techniques.) Part of the discrepancy is probably due to the assumption that only rodlike shapes are present and segmented, and kinked rods are ignored when calculating lengths from R_g values obtained from HPSEC. This assumption should become less accurate as the length of molecules decrease.

Figs. 6–9 are distributions based on numbers of aggregates. Chromatograms previously determined by HPSEC[3] with concentration detection are distributions based on weights of molecules. If one assumes that its molecular weight is proportional to the length (L) of pectin, the weight fraction (W_i) of each compo-

TABLE II

Weight fractions of pectin components

Component		Weight fraction		
Microscope	HPSEC	Microscope	Microscope	HPSEC
		Water [a]	Water–Glycerol [b]	NaCl [c]
	4			0.052
1	3	0.246 (0.199)	0.251 (0.204)	0.184
2	2	0.223 (0.228)	0.237 (0.243)	0.356
3	1	0.222 (0.239)	0.233 (0.251)	0.408
4		0.151 (0.163)	0.154 (0.166)	
5		0.094 (0.101)	0.047 (0.051)	
6		0.043 (0.046)	0.051 (0.055)	
7		0.021 (0.023)	0.027 (0.030)	

[a] Calculated from image analysis on intact microgels by assuming dissociation at T-junctions. Numbers uncorrected for aggregation not in parentheses, numbers in parentheses corrected for aggregation. Components 1–7 correspond to numbered peaks in Fig. 8. [b] Calculated from image analysis on dissociated microgels. Numbers uncorrected for aggregation are not in parentheses, while numbers corrected for aggregation are in parentheses. Components 1–7 correspond to numbered peaks in Fig. 9. [c] Measured with a refractive index detector from areas under chromatograms (see ref 3). HPSEC data taken from Table I in ref 3.

nent in Figs. 8 and 9 can be calculated from eq. *2*.

$$W_i = N_i L_i / \Sigma N_i L_i \qquad (2)$$

Table II contains the weight fractions of pectin components calculated from eq. *2*. These weight fractions decreased, whereas comparable fractions determined by HPSEC increased. Previously[3], we found that HPSEC components 3–1, had aggregation numbers (AN) of 3, 3.8, and 4 respectively. If we assign these numbers to the comparable microscope components, 1–3, and assume that the remaining components have 4 as their AN, the W_i of the components determined by microscopy and corrected for aggregation can be calculated by eq. *3*.

$$W_i = N_i L_i (AN)_i / \Sigma N_i L_i (AN)_i \qquad (3)$$

Weight fractions calculated from eq. *3* are in Table II. These calculations show that microscope component 3 and comparable HPSEC component 1 is the component with the largest weight fraction. Furthermore, the three largest HPSEC components and three smallest microscope components increase sequentially in weight fraction. The components determined by microscopy pass through a maximum with component 3, when the sequence passes from 1–7.

Global average lengths of pectin based on weight fractions corrected and uncorrected for aggregation are in Table III. In addition, lengths determined by HPSEC are in Table III. Accounting for aggregation tends to raise all global averages slightly over uncorrected values due to the effect on weight fractions of the components. Number and weight averages determined by microscopy agree more closely with equivalent HPSEC values than do Z values. Again, this may be a result of assuming that only rods are present. Compensating errors tend to give

TABLE III

Global average contour lengths [a] of pectin

	Microscope	Microscope	HPSEC
Average	Water [b]	Water–Glycerol [c]	NaCl [d]
Number	66 (70)	67 (71)	74
Weight	89 (93)	91 (95)	98
Z	121 (123)	124 (127)	134

[a] In nm. [b] Obtained from image analysis on dissociated microgels. Numbers uncorrected for aggregation are not in parentheses, while numbers corrected for aggregation are in parentheses. [c] Obtained from image analysis on intact microgels by assuming dissociation at T-junctions. Numbers uncorrected for aggregation are not in parentheses, while numbers corrected for aggregation are in parentheses. [d] Measured with a refractive index detector from areas under chromatograms. Data taken from ref 3.

better agreement between microscopy and HPSEC for all global values than might be expected when comparing values for the two methods on individual components (see Table I). Filtering of larger sized molecules in the preparation of HPSEC samples may lower the global averages, whereas the rodlike approximation may raise them. About 95% of the HPSEC preparation overlaps in length with about 70% of the molecules visualized with microscopy on a weight basis (see Table II.) Five percent of the HPSEC preparation falls below the visualization range of the microscope, whereas ~ 30% of the pectin visualized by the microscope is filtered out in preparation for HPSEC. Pectin samples from other sources often contain a larger percentage of smaller sized components than peaches[12].

We have shown that pectin microgels were held together by noncovalent forces, since they could be dissociated into macromolecular subunits by solvents such as glycerol (Fig. 3) or NaCl (Fig. 4). The question arises as to whether an appropriate solvent could dissociate macromolecular pectin subunits even further into oligomeric fragments, thus indicating that the subunits themselves were held together by noncovalent forces to some extent. To investigate this question, peach ASP was dissolved in 25 mM potassium oxalate buffer, pH 6, and chromatographed under the influence of a linear ionic gradient of the pH 6 oxalate buffer up to 500 mM on a CarboPac PA1 anion-exchange column. The chromatogram that resulted from this experiment is shown in Fig. 10a. Fig. 10b is a chromatogram of pectin from the same batch but treated with endo-polygalacturonase. Fig. 10c is a chromatogram of untreated polygalacturonic acid (Sigma, citrus). The untreated polygalacturonic acid gave virtually a continuum of oligomers with dp's[7] between 0 and 30, and a monomodal envelope that we have described previously as a "polymer" peak[13]. Since oligomeric fragments have been found to regulate physiological processes in plants[14], the faint traces of oligomeric peaks in Fig. 10a may indicate that in addition to endo-polygalacturonase activity, solvolytic changes in plant cell walls regulate metabolic processes through dissociation of oligomers from pectin. On the other hand, the artifactual production of pectic oligomers during pectin extraction is also possible. Nevertheless, alkaline-soluble

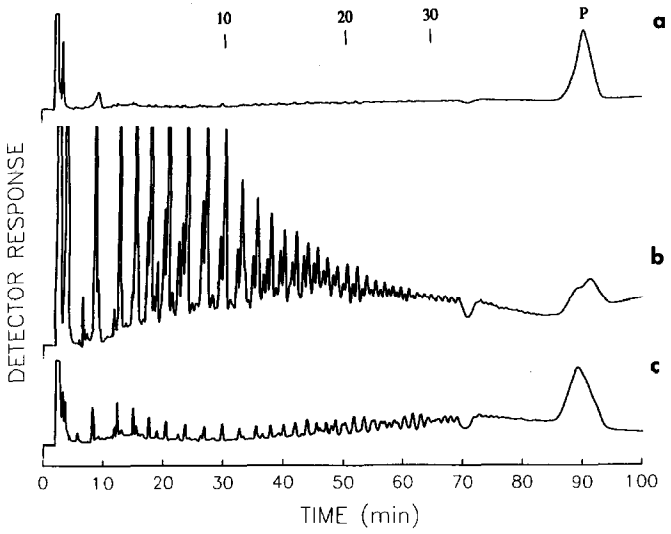

Fig. 10. High-performance anion-exchange chromatography of pectic oligosaccharides. (a) Untreated alkaline-soluble peach pectin (ASP). (b) ASP hydrolyzed with *endo*-α-D-galacturonase. (c) Potassium polygalacturonate.

pectin from peaches, which is dissociated into rods, segmented rods and kinked rods, is relatively stable to further large-scale, solvolytic dissociation, particularly when compared to tomato pectin[15]. In the case of alkaline soluble pectin extracted from isolated cell walls of mature green tomatoes, about 32% of the material dissociated into small fragments when dialyzed against 0.05 M NaCl.

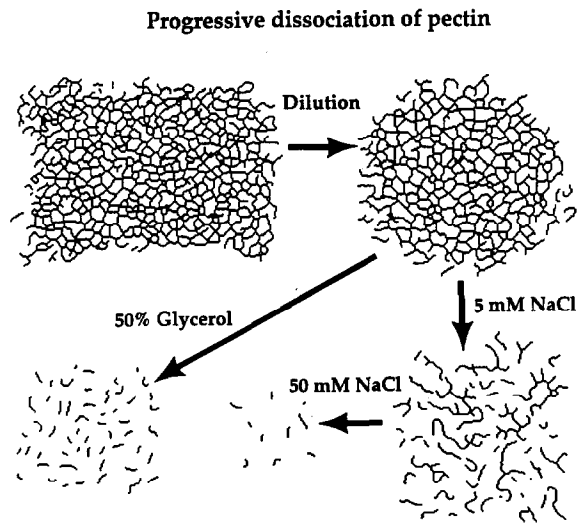

Fig. 11. Schematic diagram of the progressive dissociation of pectin.

CONCLUSIONS

Based on the foregoing experiments, we have summarized in Fig. 11 the progressive dissociation of pectin gels that were obtained by mild alkaline extraction from cell walls located in the mesocarp of melting-flesh peaches. In somewhat concentrated aqueous solutions, this pectin exists as large gel networks of indefinite shape. Dilution of these gels with water produces microscopic aggregates of pectin, some in the form of circular or spherical gels with integrated networks. The internal structure of the microgels is maintained by noncovalent forces, since the internal network can be dissociated by aqueous glycerol or salt (e.g., NaCl or $NaNO_3$) into a multimodal distribution of subunits. Subunits are comprised of pectic substances aggregated in the shape of rods, segmented rods, and kinked rods which are ~2–4 nm wide and range in length from ~20 to in excess of 300 nm. Segment length-distributions from whole and dissociated microgels are comparable, suggesting that the networks undergo solvolytical separations at T-junctions or nodes.

ACKNOWLDGEMENT

We thank Lavon Carson for technical assistance in the image analysis of pectin microgels.

REFERENCES

1 M.L. Fishman, in Y.H. Hui (Ed.), *Encyclopedia of Food Science*, Vol. 3, Wiley, New York, 1991, pp 2039–2043.
2 G.B. Fincher and B.A. Stone, in W. Tanner and F.A. Loewus (Eds.), *Plant Carbohydrates II*, Vol. 13, Springer-Verlag, New York, 1981, pp 103–105.
3 M.L. Fishman, P. Cooke, B. Levaj, D.T. Gillespie, S.M. Sondey, and R. Scorza, *Arch. Biochem. Biophys.*, 294 (1992) 253–260.
4 K.C. Gross, *Physiol. Plant.*, 62 (1984) 25–32.
5 M. Dubois, K.A. Gilles, J.K. Hamilton, P.A. Rebers, and F. Smith, *Anal. Chem.*, 28 (1956) 350–356.
6 R.W. Scott, *Anal. Chem.*, 51 (1979) 936–941.
7 L.W. Donor, P.L. Irwin, and M.J. Kurantz, *J. Chromatogr.*, 449 (1988) 229–239.
8 A.T. Hotchkiss, Jr., and K.B. Hicks, *Anal. Biochem.*, 184 (1990) 200–206.
9 W.W. Yau, J.J. Kirkland, and D.D. Bly, *Modern Size-Exclusion Chromatography*, Wiley, New York, 1979, pp 318.
10 N. Draper and H. Smith, *Applied Regression Analysis*, Wiley, New York, 1966, pp 267–270.
11 A.M. Stephen, in G.O. Aspinall (Ed.), *The Polysaccharides*, Vol. 2, Academic Press, New York, 1983, pp 158–161.
12 M.L. Fishman, Y.S. El-Atawy, S.M. Sondey, D.T. Gillespie, and K.B. Hicks, *Carbohydr. Polym.*, 15 (1991) 89–104.
13 A.T. Hotchkiss and M.L. Fishman, *Plant Physiol.*, 99 (1992) 46a.
14 C.A. Ryan and E.E. Farmer, *Annu. Rev. Plant. Physiol. Mol. Biol.*, 42 (1991) 651–674.
15 M.L. Fishman, K.C. Gross, D.T. Gillespie, and S.M. Sondey, *Arch. Biochem. Biophys.*, 274 (1989) 179–191.